Phase Diagrams of Binary Polymer Solutions and Blends

Caibao Qian, Stephen J. Mumby,* and B. E. Eichinger

BIOSYM Technologies, Inc., 10065 Barnes Canyon Road, San Diego, California 92121

Received May 7, 1990; Revised Manuscript Received August 22, 1990

ABSTRACT: A generalized Flory–Huggins theory for use in fitting and predicting liquid–liquid phase diagrams is presented. The χ parameter is defined through the chemical potential of the diluent and is represented as a product of composition-dependent and temperature-dependent terms. The former is quadratic, and the latter contains a logarithmic term in addition to the usual linear dependence on $1/T$. The Koningsveld g factor is obtained by integration of the composition-dependent χ. Comparisons are made with experimental data, and it is shown that the functional form that is chosen for χ is sufficient to fit phase diagrams having a upper and lower critical solution temperatures, combination of the two with the LCST lying above the UCST, closed loop, and hourglass shapes. Such comparisons may be used to extract the temperature and concentration dependence of χ for the system. Both binodals and spinodals are calculated. The treatment is applicable to polymer blends as well as solutions with low molecular weight diluents.

Introduction

Phase diagrams can be used to describe liquid–liquid phase separation in polymer solutions and blends. For a binary system, such diagrams are typically comprised of two phase regions: the domain of coexistence is bounded by the binodal curve, and the limits of metastability are defined by the spinodal curve. The miscible and binodal regions correspond to the existence of a single stable phase and two stable phases, respectively, and in the spinodal region the two components form two metastable phases. Undoubtably, the most well-known theory of the thermodynamics of mixing and phase separation in polymer systems is the Flory–Huggins lattice theory.[1] However, one of the major shortcomings of the original Flory–Huggins theory is that the Flory–Huggins interaction parameter (χ_{FH}) employed in this theory is considered to be concentration independent and inversely proportional to temperature. Experimentally, it is known that this is an oversimplification and that the interaction parameter is actually a much more complicated function of both concentration and temperature for most real polymer systems. In addition, the Flory–Huggins theory describes the phase separation only qualitatively rather than quantitatively.

Other theories, such as corresponding states,[2] equation of state,[3,4] and others,[5] were introduced to take account of the effect of the properties of the pure components on the interaction parameter. While these theories successfully explained both the lower critical solution temperature (LCST) and upper critical solution temperature (UCST) phenomena in some polymer systems, they have not been widely used because most of the characteristic properties of the pure components required by these theories are unknown, especially for polymer systems. An alternative approach to describe quantitatively the phase behavior of real polymer systems is to consider the interaction parameter (χ) to be a general function of both temperature and concentration (i.e., treat χ as an empirical function). This approach has the advantage that a considerable amount of data has already been published on the temperature and concentration dependence of χ[6,7] for polymer solutions, and some of this has been tabulated.[8–11] Here we describe a modeling method based on the latter approach, and we illustrate how this allows the interpretation and fitting of several experimentally observed forms of phase diagrams for binary systems. In addition to predicting the phase behavior of binary polymeric systems for which χ and its dependence on temperature and concentration is known, the method described here also permits the estimation of $\chi(T,\varphi)$ by fitting theoretical curves to experimental binodals or spinodals.

Thermodynamic Function

Free Energy of Mixing. The Flory–Huggins expression for the Gibbs free energy density of mixing of component 1 with component 2 is given by[1]

$$\frac{\Delta G}{RT} = \frac{\varphi_1}{N_1}\ln\varphi_1 + \frac{\varphi_2}{N_2}\ln\varphi_2 + \chi_{FH}\varphi_1\varphi_2 \tag{1}$$

where ΔG is the free energy of mixing per unit volume, R is the gas constant, T is the absolute temperature, φ_1 and φ_2 and N_1 and N_2 are the volume fractions and relative molar volumes of component 1 and component 2, respectively, and χ_{FH} is the Flory–Huggins interaction parameter. The volume fractions φ_1 and φ_2 of component 1 and 2 are given by

$$\varphi_1 = \frac{n_1N_1}{n_1N_1 + n_2N_2} \tag{2}$$

$$\varphi_2 = \frac{n_2N_2}{n_1N_1 + n_2N_2} \tag{3}$$

where n_1 and n_2 are the proportionate number of moles of components 1 and 2.

In eq 1, χ_{FH} is concentration independent and is only a function of the reciprocal of temperature. However, χ_{FH} should be replaced by a more general interaction parameter, $g(T,\varphi_2)$, that is dependent on both temperature and concentration, i.e.,

$$\frac{\Delta G}{RT} = \frac{\varphi_1}{N_1}\ln\varphi_1 + \frac{\varphi_2}{N_2}\ln\varphi_2 + g\varphi_1\varphi_2 \tag{4}$$

if real systems are to be described by this free energy function.

Figure 1 is a schematic representation of a typical dependence of ΔG on φ_2 at a temperature T', together with the corresponding phase diagram. At temperature T' the system is miscible for only part of the range of φ_2. The phase diagram is of the LCST type. On the phase diagram, the outer bold curve is the binodal and is defined by the points of the common tangent to ΔG (i.e., φ_a and φ_e at T'). At these compositions the chemical potentials are equal and two phases can coexist. The inner curve on

0024-9297/91/2224-1655$02.50/0

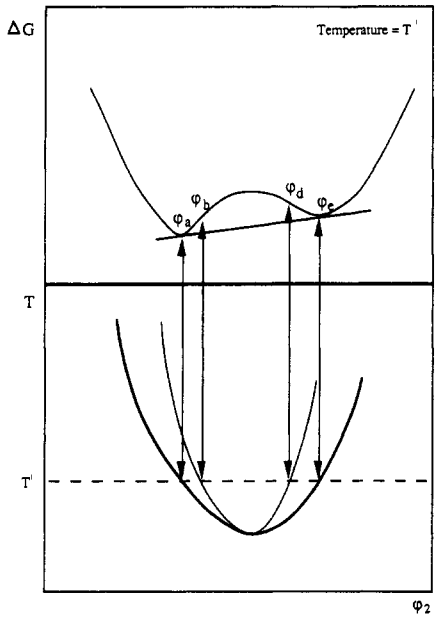

Figure 1. Schematic representation of a typical dependence of ΔG on φ_2 at temperature T' and the corresponding phase diagram (T vs φ_2).

the phase diagram in Figure 1 is the spinodal, which is defined by the points of inflection on the upper curve of ΔG (i.e., φ_b and φ_d at T'). For compositions between φ_b and φ_d the system is unstable to all small concentration fluctuations, and the phase separation process is called spinodal decomposition. Between φ_a and φ_b and φ_d and φ_e, small fluctuations are damped out and phase separation proceeds by a nucleation and growth process. The point where the binodal and the spinodal meet is the critical point.

To construct a phase diagram for a binary system, it is necessary to evaluate eq 4. However, the interaction parameter g cannot be determined directly from experiment, and it is therefore more convenient to relate g to an experimentally derivable interaction parameter χ defined in terms of chemical potentials. The relationship between g and χ is developed in the following section.

Partial Molar Quantities. The chemical potential $\Delta\mu_i$ of the component i in the solution is defined as

$$\Delta\mu_i = (\partial \Delta G/\partial n_i)_{T,P,n_j} \tag{5}$$

The following expressions for the chemical potentials of components 1 and 2 can be derived from eqs 4 and 5 as

$$\Delta\mu_1/RT = \ln(1-\varphi_2) + \varphi_2(1 - N_1/N_2) + gN_1\varphi_2^2 - \varphi_1\varphi_2^2 N_1 g' \tag{6}$$

$$\Delta\mu_2/RT = \ln\varphi_2 + (1 - N_2/N_1)(1-\varphi_2) + gN_2(1-\varphi_2)^2 + N_2\varphi_1^2\varphi_2 g' \tag{7}$$

where

$$g' = (\partial g/\partial\varphi_2)_T$$

The interaction parameter, χ, is defined[8] in terms of the chemical potential of component 1 as

$$\chi = \frac{\Delta\mu_1}{N_1 RT\varphi_2^2} - \frac{\ln(1-\varphi_2) + \varphi_2(1 - N_1/N_2)}{N_1\varphi_2^2} \tag{8}$$

Comparing eq 6 with eq 8, we have[6]

$$\chi = g - \varphi_1 g' \tag{9}$$

and on integration

$$\int_{\varphi_2}^{1}\chi(T,\varphi)\,d\varphi = (1-\varphi_2)g(T,\varphi_2) \tag{10}$$

As can be seen, g is not equal to χ in general. Only if g is independent of concentration are g and χ equal. The concentration dependence of the interaction parameter can be determined by osmotic pressure, vapor pressure, gas–liquid chromatography, freezing-point depression, swelling equilibria, intrinsic viscosity, light scattering, critical point, and other methods.[8]

It follows from eq 9 that

$$\chi' = 2g' - \varphi_1 g'' \tag{11}$$

$$\chi'' = 3g'' - \varphi_1 g''' \tag{12}$$

where the prime, double prime, and triple prime denote the first, second, and third derivatives with respect to the volume fraction of component 2.

An analysis of eqs 4, 6, 7, 9, and 10 gives the free energy and chemical potentials in terms of the interaction parameter χ as

$$\frac{\Delta G}{RT} = \frac{1-\varphi_2}{N_1}\ln(1-\varphi_2) + \frac{\varphi_2}{N_2}\ln\varphi_2 + \varphi_2\int_{\varphi_2}^{1}\chi(T,\varphi)\,d\varphi \tag{13}$$

$$\Delta\mu_1/RT = \ln(1-\varphi_2) + \varphi_2(1 - N_1/N_2) + \chi(T,\varphi_2)N_1\varphi_2^2 \tag{14}$$

$$\Delta\mu_2/RT = \ln\varphi_2 + (1 - N_2/N_1)(1-\varphi_2) - N_2\varphi_2(1-\varphi_2)\chi(T,\varphi_2) + N_2\int_{\varphi_2}^{1}\chi(T,\varphi)\,d\varphi \tag{15}$$

Selection of the Functional Form for χ. The exact analytical form of the expression for χ need not be known, but for computational expediency we will regard χ to be comprised of a product of temperature-dependent, $D(T)$, and concentration-dependent, $B(\varphi_2)$, terms,[9] such that

$$\chi = D(T)\,B(\varphi_2) \tag{16}$$

The form of the concentration dependent term is taken as[12]

$$B(\varphi_2) = b_0 + \sum_{i=1}^{n} b_i\varphi_2^{\,i} \tag{17}$$

where b_i ($i = 1, \ldots, n$) are constants (b_0 is equal to 1 in ref 12). These are the most general and realistic functional forms available in the literature,[12-19] and in addition the original concentration-independent Flory–Huggins interaction parameter may be readily recovered from these expressions. The concentration dependence of χ has been reported for certain polymer solutions, and although the amount of such information is more limited for blends, the approach here is equally applicable. Furthermore, the values of the coefficients b_i can be estimated from the experimental data of critical solution temperatures and concentrations in spinodal or binodal curves. The concentration-dependent interaction parameter function is adequately described by a second-order function in most cases, so the form

$$B(\varphi_2) = 1 + b_1\varphi_2 + b_2\varphi_2^2 \tag{18}$$

is used in our work.

To determine an appropriate functional form for $D(T)$, we start by separating $D(T)$ into enthalpy, κ, and entropy,

ψ, terms[1] as

$$D(T) = \kappa + \psi \tag{19}$$

In addition, we have the two standard thermodynamic functions

$$d(TD)/dT = \psi \tag{20}$$

$$d\psi/dT = \xi/T \tag{21}$$

where ξ is proportional to the reduced partial molar heat capacity of solution at constant pressure.

Equation 21 integrates to

$$\psi = \xi \ln T + \text{constant} \tag{22}$$

on the assumption that ξ is a constant. This expression for ψ may be substituted into eq 20 and integrated to get[13,14]

$$D(T) = d_0 + d_1/T + d_2 \ln T \tag{23}$$

where d_0, d_1, and d_2 are constants.

Phase Equilibria in Binary Systems

Binodal. Under certain thermodynamic conditions, a homogeneous polymer solution or mixture may separate into two or more phases. The conditions for equilibrium between two phases in a binary monodisperse component system may be expressed by the equations

$$\Delta\mu'_1 = \Delta\mu''_1 \tag{24}$$

$$\Delta\mu'_2 = \Delta\mu''_2 \tag{25}$$

where the prime and double prime denote two different phases. Using eqs 14, 15, 24, and 25, one obtains the expressions

$$\ln\left(\frac{1-\varphi''_2}{1-\varphi'_2}\right) + (\varphi''_2 - \varphi'_2)\left(1 - \frac{N_1}{N_2}\right) + N_1[\chi(T,\varphi''_2)\varphi''^2_2 - \chi(T,\varphi'_2)\varphi'^2_2] = 0 \tag{26}$$

$$\ln\left(\frac{\varphi''_2}{\varphi'_2}\right) + \left(1 - \frac{N_2}{N_1}\right)(\varphi'_2 - \varphi''_2) - N_2[\varphi''_2\varphi''_1\chi(T,\varphi''_2) - \varphi'_2\varphi'_1\chi(T,\varphi'_2)] + N_2\left[\int_{\varphi''_2}^{1}\chi(T,\varphi)\,d\varphi - \int_{\varphi'_2}^{1}\chi(T,\varphi)\,d\varphi\right] = 0 \tag{27}$$

Combining eqs 16, 27, and 28, we have the equations

$$\ln\left(\frac{1-\varphi''_2}{1-\varphi'_2}\right) + (\varphi''_2 - \varphi'_2)\left(1 - \frac{N_1}{N_2}\right) + N_1D(T)[B(\varphi''_2)\varphi''^2_2 - B(\varphi'_2)\varphi'^2_2] = 0 \tag{28}$$

$$\ln\left(\frac{\varphi''_2}{\varphi'_2}\right) + \left(1 - \frac{N_2}{N_1}\right) - N_2D(T)[\varphi''_2\varphi''_1B(\varphi''_2) - \varphi'_2\varphi'_1B(\varphi'_2) - \int_{\varphi''_2}^{\varphi'_2}B(\varphi)\,d\varphi] = 0 \tag{29}$$

that must be solved simultaneously to obtain the binodal curve. By giving the volume fraction in one phase for component 2, the above two equations may be solved to obtain the volume fraction in the other phase for the same component.

As can be seen, the temperature-dependent χ parameter can also be obtained easily from eqs 28 and 29. Then $D(T)$ can be inverted to get the temperature on the binodal curve.

Spinodal. The spinodal curve defines the boundary between unstable and metastable mixtures. Thermodynamically, the spinodal condition is defined by

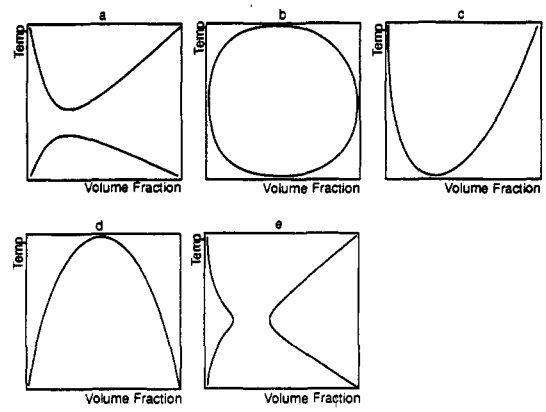

Figure 2. Effects of the coefficients d_1 and d_2 on the shape of the spinodal curve: (a) $d_2 > 0$, (b) $d_2 < 0$, (c) $d_1 < 0$ and $d_2 = 0$, (d) $d_1 > 0$ and $d_2 = 0$, and (e) $d_2 > 0$.

$$\partial^2\Delta G/\partial\varphi_1^2 = 0 \tag{30}$$

When this expression is negative, the system always separates into different phases. Explicitly, the spinodal curve is described mathematically by

$$\frac{1}{N_1\varphi_1} + \frac{1}{N_2\varphi_2} - 2g + 2(1-2\varphi_2)g' + g''\varphi_2(1-\varphi_2) = 0 \tag{31}$$

By substituting g' and g'' from eqs 10 and 11 into the above equation, one obtains

$$\frac{1}{N_1(1-\varphi_2)} + \frac{1}{N_2\varphi_2} - 2\chi(T,\varphi_2) - \varphi_2\chi'(T,\varphi_2) = 0 \tag{32}$$

Upon substituting eq 16 into eq 32, one finds

$$\frac{1}{N_1(1-\varphi_2)} + \frac{1}{N_2\varphi_2} - [2B(\varphi_2) + \varphi_2B'(\varphi_2)]D(T) = 0 \tag{33}$$

To understand the conditions for incipient spinodal phase separation, let us analyze eq 33 for different cases. For the convenience of analysis, define Z as

$$Z = 2B(\varphi_2) + \varphi_2B'(\varphi_2) \tag{34}$$

It is clear from eq 33 that Z and $D(T)$ must have the same sign for the equation to possess a solution. First note that

$$\frac{dD(T)}{dT} = -\frac{d_1}{T^2} + \frac{d_2}{T} \tag{35}$$

$$\left.\frac{d^2D(T)}{dT^2}\right|_{T=T^*} = \frac{d_2}{T^{*2}} \tag{36}$$

The extremal temperature obtained by setting eq 35 equal to zero is

$$T^* = d_1/d_2 \tag{37}$$

The slope and curvature of $D(T)$ determine the shape of the phase diagram. Conditions for phase separation are readily deduced from inspection of eq 33 with the aid of eqs 35–37. If this equation is satisfied, we may have two kinds of phase diagrams of temperature versus concentration depending on the sign of d_2. Both LCST and UCST phenomena may exist in principle. When d_2 is positive, a phase diagram such as in Figure 2a is obtained, and when d_2 is negative, one similar to that in Figure 2b is found. However, one should not be surprised to observe only either LCST or UCST behavior in a certain experimental temperature range. If d_2 is equal to 0, only an

LCST or a UCST can be observed (Figure 2c,d), depending on the sign of d_1. Figure 2e is obtained when the UCST and LCST (as in Figure 2a) boundaries coalesce so that the two regions of limited miscibility give an hourglass shape. No critical temperature is present in this case. On the other hand, if Z and $D(T)$ have opposite signs, the system is stable and no phase separation occurs.

Critical Point. The critical point is on the binodal and spinodal curves where the two phases become identical and form one phase. This condition is expressed as

$$\frac{\partial \Delta\mu_1}{\partial \varphi_2} = \frac{\partial^2 \Delta\mu_1}{\partial \varphi_2^2} = 0 \tag{38}$$

Explicitly, these conditions are

$$\frac{1}{1-\varphi_2} + \left(\frac{N_1}{N_2} - 1\right) - 2gN_1\varphi_2 + 2N_1\varphi_2(1-2\varphi_2)g' + \varphi_2^2(1-\varphi_2)N_1 g'' = 0 \tag{39}$$

$$\frac{1}{(1-\varphi_2)^2} + 2gN_1 + (10\varphi_2 - 2)N_1 g' + \varphi_2(7\varphi_2 - 4)g''N_1 - \varphi_2^2(1-\varphi_2)N_1 g''' = 0 \tag{40}$$

After substituting eqs 10–12 and 16 into eqs 39 and 40, one obtains

$$\frac{1}{1-\varphi_2} - \left(1 - \frac{N_1}{N_2}\right) - N_1\varphi_2[\varphi_2 B'(\varphi_2) + 2B(\varphi_2)]D(T) = 0 \tag{41}$$

$$-\frac{1}{(1-\varphi_2)^2} + N_1[2B(\varphi_2) + 4\varphi_2 B'(\varphi_2) + \varphi_2^2 B''(\varphi_2)]D(T) = 0 \tag{42}$$

One solves the above two equations simultaneously to get the critical temperature and critical volume fraction.

Examples of Phase Diagrams

In polymer solutions and polymer blends, LCST, UCST, combined USCT and LCST, hourglass, and closed-loop shaped phase diagrams have been found experimentally. These five types of phase diagrams are the most commonly observed phase diagrams in polymer systems. Polystyrene in cyclohexane exhibits a UCST phase diagram,[12] whereas polystyrene in benzene exhibits an LCST-type phase diagram.[12] However, polystyrene in acetone may exhibit either a combined UCST and LCST type or an hourglass shape phase diagram, depending on the molecular weight of the polystyrene.[17] A closed-loop phase diagram is found in the poly(vinyl alcohol)–water system.[20] Recently, a closed-loop phase diagram was also reported for polycarbonate and poly(methyl methacrylate) blends,[21] but a reviewer has brought to our attention that this work is flawed by kinetic artifacts due to the use of finite heating rates. The majority of known compatible polymer blends exhibit LCST type phase diagrams, but some examples of UCST type behavior are known, such as the polybutadiene and poly(methylstyrene) system.[23] Polybutadiene and poly(styrene-*co*-butadiene) blends give a combined UCST and LCST type phase diagram.[24] According to Sanchez,[25] 95% of binary blends have phase diagrams of the hourglass shape and are incompatible over much of the range of composition. A detailed description of phase diagrams and the compatibility of polymer blends and solutions can be found in the literature.[22,26]

Hypothetical Phase Diagrams. As stated in the above section, the theory described here is capable of representing phase diagrams of the UCST, LCST, combined UCST and LCST (with the UCST below the LCST), hourglass, and closed loop (with the UCST above LCST). To generate a phase diagram of a particular form, one should start by adjusting the coefficients (b_1 and b_2) of the concentration-dependent interaction parameter until the desired critical volume fraction is obtained. This may be assessed by viewing a plot of χ against φ_2, the former being the locus of points that solves the equilibrium equations. The coefficients (d_0, d_1, and d_2) of the temperature-dependent interaction parameter may then be used to adjust the shape of the phase diagram (T against φ_2). We find it expedient to begin by setting d_0 in the range ±0.5 and then a guide for the initial values of d_1 and d_2 may be obtained from Table I. Small changes may then be made to the values of the coefficients to optimize the phase diagram to the required form. The χ interaction parameter thus obtained is taken to be the true interaction parameter for the system.

To illustrate the generation of the different phase diagrams, five phase diagrams were produced for hypothetical polymer blends by using the functions for χ shown in Table II. The resulting phase diagrams are displayed in Figure 3. The molecular weights of components 1 and 2 are 10^4 and 10^6, respectively. The density of both components is 1.00 g cm^{-3}. The degree of polymerization of component 1 is 100.

As one can see from Figure 3, the theory discussed here is able to predict five types of phase diagrams in polymer

Table I
Effect of d_1 and d_2 on the Type of Phase Diagram

d_1	d_2	type of phase diagram
>0	0	UCST
<0	0	LCST
>0	>0	LCST + UCST, hourglass
<0	<0	closed loop

Table II
Interaction Parameters Used To Generate the Hypothetical Phase Diagrams of Polymer Blends Shown in Figure 4

$\chi(T,\varphi)$	type of phase diagram
$(1 + 0.01\varphi_2 + 0.001\varphi_2^2)(0.013 - 2.01/T)$	LCST
$(1 + 0.01\varphi_2 + 0.001\varphi_2^2)(0.0 + 2.01/T)$	UCST
$(1 + 0.01\varphi_2 + 0.001\varphi_2^2)(-0.03487 + 2.01/T + 0.006 \ln T)$	combined UCST and LCST
$(1 + 0.01\varphi_2 + 0.001\varphi_2^2)(-0.03435 + 2.01/T + 0.006 \ln T)$	hourglass
$(1 + 0.01\varphi_2 + 0.001\varphi_2^2)(0.047 - 2.01/T - 0.006 \ln T)$	closed loop

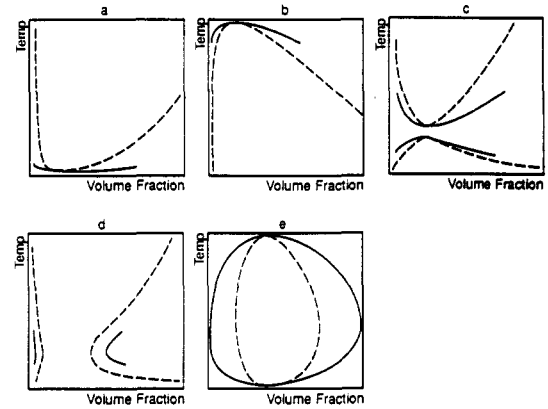

Figure 3. Phase diagrams of hypothetical polymer blends. The solid line is the binodal and the broken line is the spinodal. The diagrams are of the form (a) LCST, (b) UCST, (c) combined LCST and UCST, (d) hourglass, and (e) closed loop.

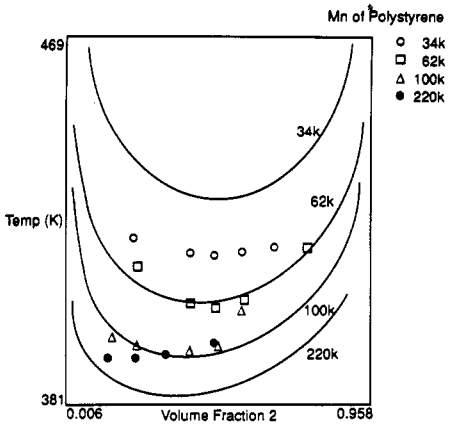

Figure 4. Experimental (points) and theoretical (curves) phase diagrams of polystyrene (M_n = 34 000, 62 000, 100 000, and 220 000) and poly(vinyl methyl ether) blends.

blends with appropriately selected interaction parameters. Similar types of phase diagrams may of course be generated for polymer solutions.

Comparison with Published Experimental Data. It has been reported that a blend of polystyrene (PS) and poly(vinyl methyl ether) (PVME) shows an LCST type phase diagram.[27] The phase diagram determinations were performed on samples of narrow molecular weight distribution in order to reduce polydispersity effects. The experimental phase diagrams of PVME (M_n = 75 000, M_w/M_n = 1.27) with four different fractions of PS (M_n = 220 000, 100 000, 62 000, and 34 000, $M_w/M_n < 1.08$) are replotted in Figure 4. The theoretical binodal curves of the different molecular weight combinations have been calculated by using a single χ interaction parameter and are also plotted in this figure. Polystyrene is component 2. The χ interaction parameter used is

$$\chi(T,\varphi_2) = (1 - 0.4\varphi_2)(0.02215 - 8.0/T) \quad (43)$$

As we can see, the calculated curves provide good fits to the experimental data corresponding to PS samples of two molecular weights (M_n = 62 000 and 100 000). However, the fitting is not as good for the other two samples (M_n = 34 000 and 220 000). This indicates that other parameters, such as the molecular weight, polydispersity, and density change, may also affect the interaction parameter in this system. Of course, different χ interaction functions may be used to fit each curve if desired.

Spinodal data have been reported[28] for blends of deuterated polystyrene (PSD) and poly(vinyl methyl ether) (PVME). The weight average molecular weights and polydispersities of the samples studied are listed in Table III. The densities of PSD and PVME at 420 K are taken as[29,30] 1.092 and 0.983 g cm^{-3}, respectively. The experimental data and the calculated spinodal curves are plotted in Figure 5 with PSD as component 2. The interaction parameters used for samples L, M, and H were

$$\chi(T,\varphi_2) = (1 - 1.5\varphi_2 + 0.815\varphi_2^2)(0.02754 - 9.0/T) \quad (44)$$

$$\chi(T,\varphi_2) = (1 - 1.5\varphi_2 + 0.815\varphi_2^2)(0.0436 - 18.0/T) \quad (45)$$

$$\chi(T,\varphi_2) = (1 - 1.5\varphi_2 + 0.815\varphi_2^2)(0.00644 - 2.5/T) \quad (46)$$

respectively. In all cases, the χ parameter required to produce an acceptable fit to the experimental data had a strong concentration dependence. The agreement between

Table III
M_w and M_w/M_n of PSD and PVME

	PSD		PVME	
	$10^{-5}M_w$	M_w/M_n	$10^{-5}M_w$	M_w/M_n
L	2.30	1.14	3.89	1.25
M	4.02	1.42	2.10	1.32
H	5.93	1.48	11.0	1.26

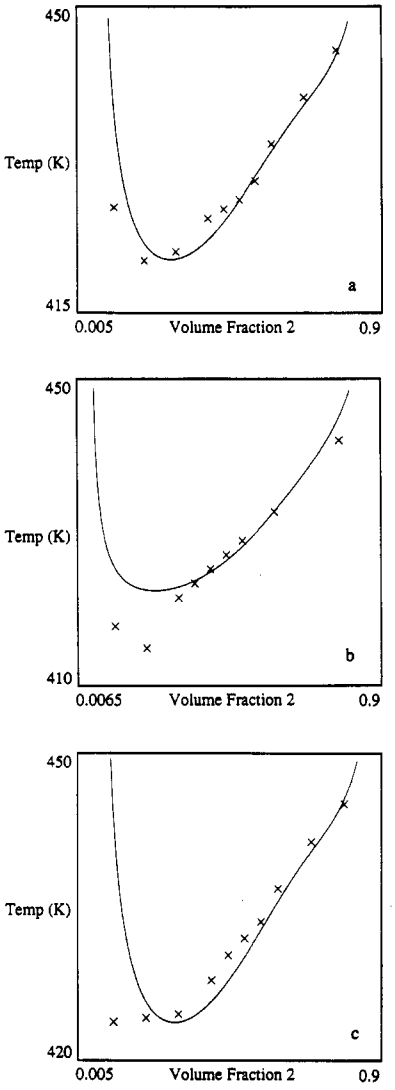

Figure 5. Experimental (points) and theoretical (curves) spinodals for blends of deuterated polystyrene and poly(vinyl methyl ether): (a) sample L, (b) sample M, and (c) sample H. (See Table III.)

calculated curves and experimental data is much better for samples L and H than for sample M. It may be pertinent to note that unlike samples L and H, sample M did not have antioxidant added to help prevent degradation.[28]

A blend of deuterated polybutadiene (DPBD) (M_n = 134 000, M_w/M_n = 2.0) and protonated polybutadiene (PBD) (M_n = 135 000, M_w/M_n = 1.8) was investigated by Sakurai et al.[31] using small-angle neutron scattering and was found to exhibit a UCST-type spinodal phase diagram. This example provides a particularly clear illustration of the advantages of determining the temperature and concentration response of the χ parameter using the method described in this publication, compared with other methods of data analysis such as those used by Sakurai et al.[31] These authors[31] used a Flory-type temperature-dependent interaction parameter such that eqs 18 and 23

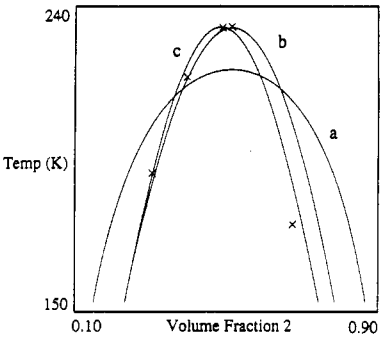

Figure 6. Experimental (points) and theoretical phase diagrams of a deuterated polybutadiene and protonated polybutadiene blend. Curve a is calculated according to the average of the experimentally determined interaction parameters. Curve b results from a temperature-dependent interaction parameter derived here, and curve c has a concentration-dependent component.

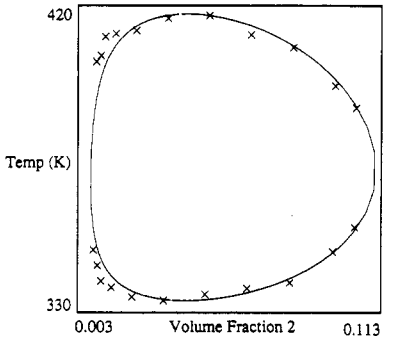

Figure 7. Experimental (points) and theoretical (curve) phase diagrams of an aqueous solution of the copolymer poly(vinyl alcohol)$_{93}$-*co*-(vinyl acetate)$_7$) (M_n = 140 000).

become

$$B(\phi_2) = 1 \tag{47}$$

$$D(T) = d_0 + d_1/T \tag{48}$$

and fitted to data at each concentration. This resulted in values of d_0 and d_1 corresponding to the different concentrations that differed in some nonsystematic way by a factor of 2–3. The variation in the values of these coefficients is presumably due to experimental uncertainty and indeed, the authors[31] state that they detected no significant composition dependence of the interaction parameter within experimental error and the range of the data. However, if one now wishes to describe the spinodal curve, it is unclear what temperature dependence to use for χ. To illustrate this point, the experimental spinodal data[31] for the DPBD/PBD blend are plotted in Figure 6 together with three theoretical curves. The deuterated polybutadiene fraction is component 2. Curve a was obtained by using average values for d_0 (=0.000 877) and d_1 (=0.295) calculated from the data in ref 31. This curve has a poor correspondence to the experimental data. However, a much better fit to the data is obtained by considering all the points simultaneously by using the approach described here. This resulted in curve b by using

$$\chi(T) = 2.20 \times 10^{-5} + 0.100/T$$

as the temperature dependent interaction parameter. This curve provides a much better fit to the experimental data. The critical volume fraction of DPBD determined by using the above concentration-independent, temperature-dependent interaction parameter is 0.501, which is identical

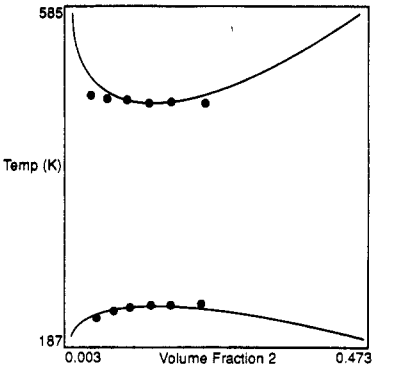

Figure 8. Experimental (points) and theoretical (curve) phase diagrams of polystyrene (M_w = 4800) in acetone.

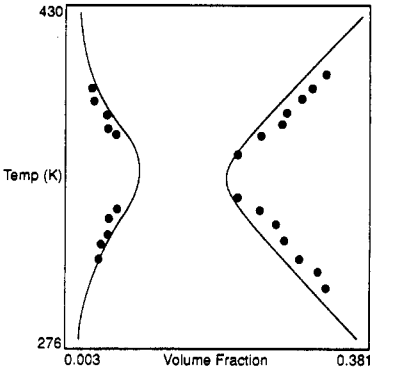

Figure 9. Experimental (points) and theoretical (curve) phase diagrams of polystyrene (M_w = 19 800) in acetone.

with that determined experimentally.[31] A slight improvement in the fit may be produced by including a concentration dependence of χ such that

$$\chi(T,\varphi_2) = (1 - 0.150\varphi_2)(0.0001195 + 0.090/T)$$

The spinodal curve that results from this concentration dependent χ is labeled c in Figure 6.

A closed-loop phase diagram is observed[20] for an aqueous solution of the copolymer poly((vinyl alcohol)$_{93}$-*co*-(vinyl acetate)$_7$) with a number average molecular weight of 140 000. This phase diagram is replotted in Figure 7 together with the theoretically fitted binodal curve. With the polymer as component 2, the interaction parameter used to generate the theoretical plot is

$$\chi(T,\varphi_2) = (1 + 0.65\varphi_2)(2.582 - 111.9/T - 0.30 \ln T)$$

It can be seen in Figure 7 that the experimental data are well represented by this expression for the interaction parameter.

A combined LCST and UCST type of phase diagram is observed for polystyrene (M_w = 4800 and 10 300, M_w/M_n = 1.06) in acetone.[17] The experimentally determined phase diagram of PS with molecular weight 4800 is replotted in Figure 8. The theoretically fitted binodal curve is also plotted in the same figure. Polystyrene is component 2. The interaction parameter is

$$\chi(T,\varphi_2) = (1.0 + 0.2\varphi_2)(-6.8829 + 345.5/T + 1.1 \ln T)$$

As we can see from Figure 8, the theoretically fitted UCST curve agrees well with the experimentally measured UCST curve. However, the correlation between theoretically fitted and the experimentally measured LCST curve is not so good.

An hourglass phase diagram is observed for polystyrene (M_w = 19 800, M_w/M_n = 1.06) in acetone.[17] The experimentally determined phase diagram is replotted in Figure

9 together with the theoretically fitted binodal curve. Polystyrene is again component 2. The interaction parameter that best fits the data is

$$\chi(T,\varphi_2) = (1.0 + 0.653\varphi_2)(-6.9933 + 376.2/T + 1.1 \ln T)$$

As can be seen from the figure, the theoretically fitted curve agrees well with the experimentally measured curve.

Conclusions

A temperature- and concentration-dependent interaction parameter has been employed to study the phase diagrams of binary monodisperse polymer solutions and blends. This approach permits the fitting of the five most generally observed types of phase diagrams by adjusting the temperature- and concentration-dependent coefficients. Thus, the interaction parameter is obtained when a best fit between the theoretically calculated and experimentally determined values is generated. Work is in progress to extend this theory to include the effects of polydispersity. The form of the free energy function used here may be extended to include thermal expansion, pressure, molecular weight, and other dependencies. At present, these elaborations do not seem to be required to obtain a good theoretical representation for observed phase behavior.

Acknowledgment. We gratefully acknowledge the graphic and interface support by Mr. Peter Sher, Ms. Patty Degen, Mr. Steve Miller, and other members of the Polymer Project staff at BIOSYM Technologies, Inc.

References and Notes

(1) Flory, P. J. *Principles of Polymer Chemistry*; Cornell University Press: Ithaca, NY, 1953.
(2) Patterson, D. *Rubber Chem. Technol.* **1967**, *40*, 1.
(3) Eichinger, B. E.; Flory, P. J. *Trans. Faraday Soc.* **1968**, *64*, 2035.
(4) Sanchez, I. C.; Lacombe, R. H. *J. Phys. Chem.* **1976**, *80*, 2352, 2568.
(5) Yamakawa, H. *Modern Theory of Polymer Solutions*; Harper & Row: New York, 1971.
(6) Koningsveld, R.; Staverman, A. J. *J. Polym. Sci., Part A-2* **1968**, *6*, 305, 325, 349.
(7) Riedl, B.; Prud'homme, R. E. *J. Polym. Sci., Polym. Phys. Ed.* **1988**, *26*, 1769.
(8) Orwoll, R. J. *Rubber Chem. Technol.* **1977**, *452*, 50.
(9) Barton, A. F. M. *Handbook of Solubility Parameters and Other Cohesion Parameters*; CRC Press: Boca Raton, FL, 1983.
(10) Barton, A. F. M. *Handbook of Polymer–Liquid Interaction Parameters and Solubility Parameters*; CRC Press; Boca Raton, FL, 1990.
(11) Brandrup, J.; Immergut, E. H. *Polymer Handbook*, 3rd ed.; Wiley: New York, 1989.
(12) Kamide, K.; Matsuda, S.; Saito, M. *Polym. J.* **1985**, *17*, 1013.
(13) Eichinger, B. E. *J. Chem. Phys.* **1970**, *53*, 561.
(14) Koningsveld, R.; Kleintjens, L. A.; Schultz, A. R. *J. Polym. Sci., A-2* **1970**, *8*, 1262.
(15) Kamide, K.; Matsuda, S. *Polym. J.* **1984**, *16*, 807.
(16) Kamide, K.; Miyazaki, Y.; Abe, T. *Polym. J.* **1982**, *14*, 335.
(17) Siow, K. S.; Delmas, G.; Patterson, D. *Macromolecules* **1972**, *29*, 5.
(18) Matsuda, S. *Polym. J.* **1986**, *18*, 993.
(19) French, D. M. *J. Polym. Sci., Part C: Polym. Lett.* **1988**, *26*, 469.
(20) Elias, H. G. *Macromolecules*, 1st ed.; Plenum Press: New York 1983; Vol. 1, p 233.
(21) Kyu, T.; Lin, D. *J. Polym Sci., Part C* **1989**, *27*, 421.
(22) Paul, D. R., Newman, S., Eds. *Polymer Blends*; Academic Press: New York, 1978; Vol. I.
(23) Lin, J. L.; Roe, R. J. *Macromolecules* **1987**, *20*, 2168.
(24) Ougizawa, T.; Inoue, T.; Kammer, H. W. *Macromolecules* **1985**, *18*, 2089.
(25) Sanchez, I. C. *Annu. Rev. Mater. Sci.* **1983**, *13*, 387.
(26) Krause, S.; Li, P. *A Polymer-Polymer Miscibility Database*; Presented at the 1989 International Chemical Congress of Pacific Basin Society Meeting, Honolulu, HI, Dec 1989.
(27) Walsh, D. J.; Dee, G. T.; Halary, J. L.; Ubiche, J. M.; Millequant, M.; Lesec, J.; Monnerie, L. *Macromolecules* **1989**, *22*, 3395.
(28) Han, C. C.; Bauer, B. J.; Clark, J. C.; Muroga, Y.; Matsushita, Y.; Okada, M.; Tran-cong, Q.; Chang, T.; Sanchez, I. C. *Polymer* **1988**, *29*, 2002.
(29) Höcker, H.; Blake, G. J.; Flory, P. J. *Trans. Faraday Soc.* **1971**, *67*, 2251.
(30) Shiomi, T.; Hamada, F.; Nasako, T.; Yoneda, K.; Imai, K.; Nakajima, A. *Macromolecules* **1990**, *23*, 229.
(31) Sakurai, S.; Hasegawa, H.; Hashimoto, T.; Hargis, I. G.; Aggarwal, S. L.; Han, C. C. *Macromolecules* **1990**, *23*, 451.